Liquid Crystals

ISSN: 0267-8292 (Print) 1366-5855 (Online) Journal homepage: http://www.tandfonline.com/loi/tlct20

The N_{TB} phase in an achiral asymmetrical bent-core liquid crystal terminated with symmetric alkyl chains

Sithara P. Sreenilayam, Vitaly P. Panov, Jagdish K. Vij & Govindaswamy Shanker

To cite this article: Sithara P. Sreenilayam, Vitaly P. Panov, Jagdish K. Vij & Govindaswamy Shanker (2017) The N_{TB} phase in an achiral asymmetrical bent-core liquid crystal terminated with symmetric alkyl chains, Liquid Crystals, 44:1, 244-253, DOI: 10.1080/02678292.2016.1253878

To link to this article: https://doi.org/10.1080/02678292.2016.1253878

Published online: 17 Nov 2016.

LIQUID CRYSTALS, 2017
VOL. 44, NO. 1, 244–253
http://dx.doi.org/10.1080/02678292.2016.1253878

Taylor & Francis
Taylor & Francis Group

INVITED ARTICLE

The N_{TB} phase in an achiral asymmetrical bent-core liquid crystal terminated with symmetric alkyl chains

Sithara P. Sreenilayam[a], Vitaly P. Panov[a], Jagdish K. Vij[a] and Govindaswamy Shanker[b]

[a]Department of Electronic and Electrical Engineering, Trinity College Dublin, The University of Dublin, Dublin, Ireland; [b]Department of Studies in Chemistry, Bangalore University, Bangalore, India

ABSTRACT

The characteristics of the twist-bend nematic (N_{TB}) phase of an achiral asymmetrical rigid bent-core liquid crystal (LC), the ends of which are terminated by symmetric alkyl chains, are reported. The nematic–nematic phase transition and its properties are studied by differential scanning calorimetry (DSC), polarising microscopy and the electro-optic techniques. Large domains of opposite handedness are observed in the absence of the external field in the N_{TB} phase. Another set of periodic striped pattern consisting of domains with sharp boundaries is formed when a high-frequency electric field with a magnitude above its threshold is applied across a planarly aligned cell. The neighbouring domains are of opposite chirality. The temperature dependence of the heliconical angle θ_0 is determined from the birefringence measurements using Haller's extrapolation technique. This material shows lower values of the heliconical angle (~9.3° at a temperature of 155°C within the N_{TB} phase) when compared with the previously reported dimer-based twist-bend nematic LCs (31°±3°).

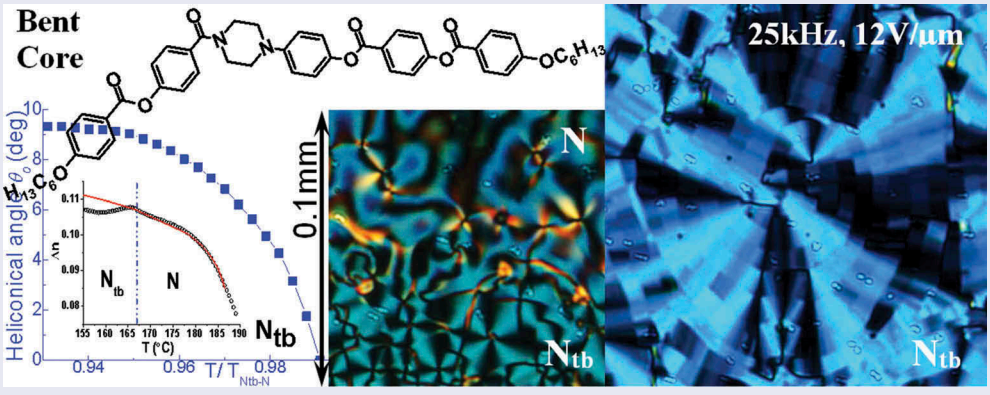

ARTICLE HISTORY
Received 22 June 2016

KEYWORDS
Bent-core liquid crystals; twist-bend nematic phase; birefringence; textures

1. Introduction

The twist-bend nematic phase (N_{TB}) provides a structural link between the conventional nematic (N) and the cholesteric nematic phase (N*) [1]. In the latter, a helical structure results from the local molecular directors confined on to a helicoid at right angle to the helicoidal axis. In the N_{TB} phase, the director makes with the axis of the helix an angle $0 < \theta_0 < \pi/2$ called the heliconical angle. It is known for 6 years now that some dimers exhibit two nematic phases, where the lower temperature phase is identified as the N_{TB}. The high-temperature phase is the conventional nematic phase though it does have some special characteristics too. In the earlier works, the low-temperature nematic phase was referred to as the N_x [2–5] phase though it was first pointed out by Panov et al. [4] that N_x phase has many unusual characteristics. It has been shown that a helicoidal structure is present with a pitch of much lower wavelength than the optical ones [2]. The nanoscale helical modulation was exactly determined by freeze fracture transmission electron microscopy (FFTEM) [1,6]. The helicoidal structure was found from 'Bouligand arches' appearing on the FFTEM images [1] and by the atomistic computer simulations carried out by Chen et al. [6]. The molecules forming the N_{TB} phase are achiral and normally the chiral domains of macroscopic sizes (tens to hundreds of μm) of both handedness are separated by domain

CONTACT Jagdish K. Vij jvij@.tcd.ie Department of Electronic and Electrical Engineering, Trinity College Dublin, The University of Dublin, Dublin 2, Ireland

boundaries [2] in this phase. This phase was predicted to exist by R. B. Meyer [7] for chiral systems and by Dozov [8] for achiral bent-core systems. It may be remarked that no one from the current liquid crystal (LC) community was really looking at these predictions and when observations of special characteristics were noted then the past literature was examined for clues. One of the major points of attention to the N_{TB} phase was drawn by the occurrence of the self-deformation patterns (periodic stripes) whose periodicity is determined by the sample geometry [4] and by the existence of large chiral domains of opposite handedness in an otherwise achiral system. It has also been demonstrated that a variety of hierarchical self-deformation patterns/structures are formed. The dimensions of these structures are found to extend from nanometre to micrometre scales [9].

Initially, the N_{TB} phase was discovered [1,4,6,10–11] in dimer-based systems where the liquid crystalline material is made up of two mesogenic cores linked to each other by a flexible hydrocarbon spacer with an odd number (n) of methylene groups. Sepej et al identified the low temperature phase in a dimeric system with an odd number of carbon atoms as columnar nematic phase [12]. The low temperature phase in a polymer system was identified as nematic by Griffen and Britt [13]. In dimers of cyanobiphenyls, the low temperature phase was identified as smectic [14–16]. It may be stated here that none of the investigators prior to 2010 [4] reported any special characteristics of the low or high temperature nematic phase. This is a crucial point to make here while discussing the discovery of twist-bend nematic phase. Though the phase has been predicted to exist for the bent-core mesogens by Dozov, N_{TB} phase has unambiguously proven to exist only in a few bent-core systems investigated so far [17]. It remains to be determined as to why the bent-core mesogens in general rarely exhibit this phase. It is quite plausible that the linking unit between the two mesogens must be flexible enough so as to form a helicoidal structure which is not the case in the bent-core systems. In this case, (i) the molecular shape of the bent-core is asymmetrical in such a way that the resulting bimesogen may bend and twist at the same time to minimise the free energy. For example, one of its arms contains only two phenyl rings, whereas the second one contains three phenyl rings and one piperazine ring and (ii) the chemical units in the bent-core systems that constitute the mesogen do not have different polarisabilities (induced dipole moment per unit electric field) as the dimers do. The polarisability of the alkyl spacer is very different from that of the substituted benzene rings.

A detailed investigation of the characteristics of the N and N_{TB} phases of the LC constituted from the rigid bent-core asymmetrical mesogen (Figure 1) is made by differential scanning calorimetry (DSC), polarised optical microscopy, and electro-optic spectroscopy. A series of compounds based on the mesogen were initially synthesised by Schröder et al. [18] where they varied the chain lengths n from 4 to 16 (Figure 1). They proposed that for $n < 7$, an unusual nematic-to-nematic phase transition occurs. The molecules in the lower temperature nematic phase are possibly stacked in the bend direction. They form bundles of undefined lengths and were suggested to act as 'precursor of the columnar phase'. Chen et al. [17] however showed using X-rays, birefringence mapping and the FFTEM, that this phase is the characteristic N_{TB} phase but a columnar phase is formed at lower temperatures than for this phase. The objective of our work is to determine what features, if any, distinguish this twist-bend phase in a bent-core system from those already observed in the dimers. We also extend the investigations of Chen et al. [17] by subjecting the LC samples to external electric fields and by studying the electroclinic effect. The switching behaviour is also being studied by making a detailed electro-optic investigation. The periodic striped domains of opposite handedness [3] are generated by applying a large high-frequency electric field in the N_{TB} phase. The temperature dependence of the conical angle θ_0 with respect to the helical axis in this phase is determined from measurements of the birefringence, Δn, using the Haller's extrapolation technique. This bent-core material shows relatively small values of the heliconical angle θ_0 (~9.3° at 155°C) as opposed to $\theta_0 = 31° \pm 3°$ found for dimers.

2. Experimental

The two arms of the synthesised compound are asymmetric and these are terminated with n-alkyl chains with the group, OC_6H_{13} (Figure 1). This compound exhibits different phase sequences under cooling and heating. On cooling, it shows Iso 190°C N 166°C N_{TB} 150°C Col 129°C Cr. On heating, it goes from the crystalline state as follows: Cr 166°C N 191°C Iso. The N_{TB} phase is exhibited only under cooling and hence is monotropic.

The enthalpies of activation associated with the phase transitions are obtained from DSC thermograms (Figure 1(b)). These are recorded using a Perkin-Elmer DSC7 calorimeter (heating and cooling rates are 10°C min^{-1}). The peak at the N–N_{TB} transition indicates a much smaller enthalpy of activation value (0.1 J/g)

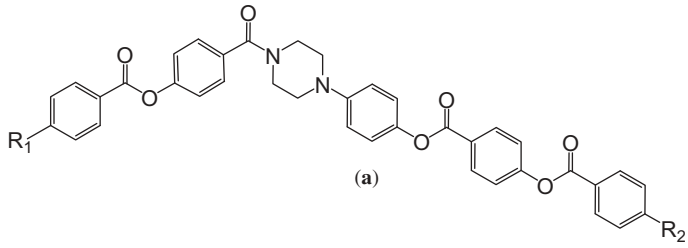

R1=R2=OC_nH_{2n+1}; n = 6

Cr 129 ºC (-23.98 J/g) Col 150 ºC (-7.04 J/g) N_{TB} 166 ºC (-)N 190 ºC (-0.33 J/g) Iso

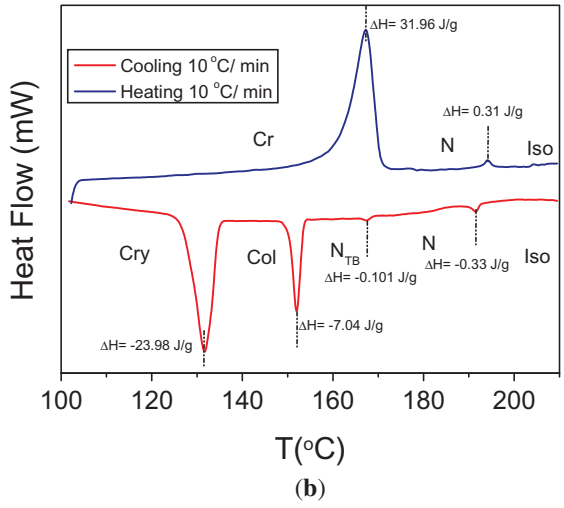

Figure 1. (Colour online). (a) The molecular structure, phase sequences and the transition temperatures [T (°C)] with enthalpies (Δ*H* [J/g] in brackets) of the achiral bent-core LC. (b) DSC heating and cooling curves (10°C min^{-1}). The phase transition temperatures are obtained on cooling under quasi-equilibrium condition with a rate of ~1°C min^{-1} using polarising optical microscopy, whereas Δ*H* is taken from the DSC cooling curves. Here, Iso implies the isotropic phase, N is the Nematic, and N_{TB} is the twist-bend nematic phase, Col refers to the columnar phase and Cr refers to the crystalline state.

when compared with a large value (2.46 J/g) for CBC7CB dimer.

Experiments are carried out on LC cells of both configurations: planar and homeotropic. The planar alignment is achieved by coating ITO glass substrates of the cell with RN1175 (Nissan Chemicals, Japan). The alignment layer on the substrates is baked at a temperature of 250°C for 30 min. The homeotropic alignment is achieved by coating the substrates with polymer AL60702 (JSR, Korea) and baking these at a temperature of 210°C for 15 min. The gap between the ITO glasses is controlled by Mylar spacers and the cell thickness is measured optically using an optical interference technique. The textures are recorded using polarising optical microscope (Olympus BX 52), connected to a digital camera and photodiode detector system (Hamamatsu C6386). The cell is mounted in the hot stage interfaced to a temperature controller (Eurotherm 2604). To study the electro-optic behaviour, voltage signal from the waveform generator (Agilent 33120A) amplified by a high-voltage amplifier (TReK PZD700) is applied across the cell under investigation.

2.1 Polarising optical microscopy

Figure 2 presents the polarising optical microphotographs in planar (a–c) and homeotropic (d–f) cells filled with the material under investigation. These textures are recorded during the cooling process from the isotropic state to temperatures of the columnar phase in the absence of an external electric field. A planar cell is positioned at an angle of α = 23°. Here, α is the angle between the rubbing direction, ***R***, and the polariser axis, ***P***.

At a temperature of 188°C (Figure 2(c,f)), the textures of both aligned cells: planarly and homeotropically correspond typically to that of the conventional uniaxial nematic phase. On cooling, the planarly aligned cell to a temperature of 166°C, its uniform texture transforms to striped one. This is one of the characteristic features of the N_{TB} phase (Figure 2(b))

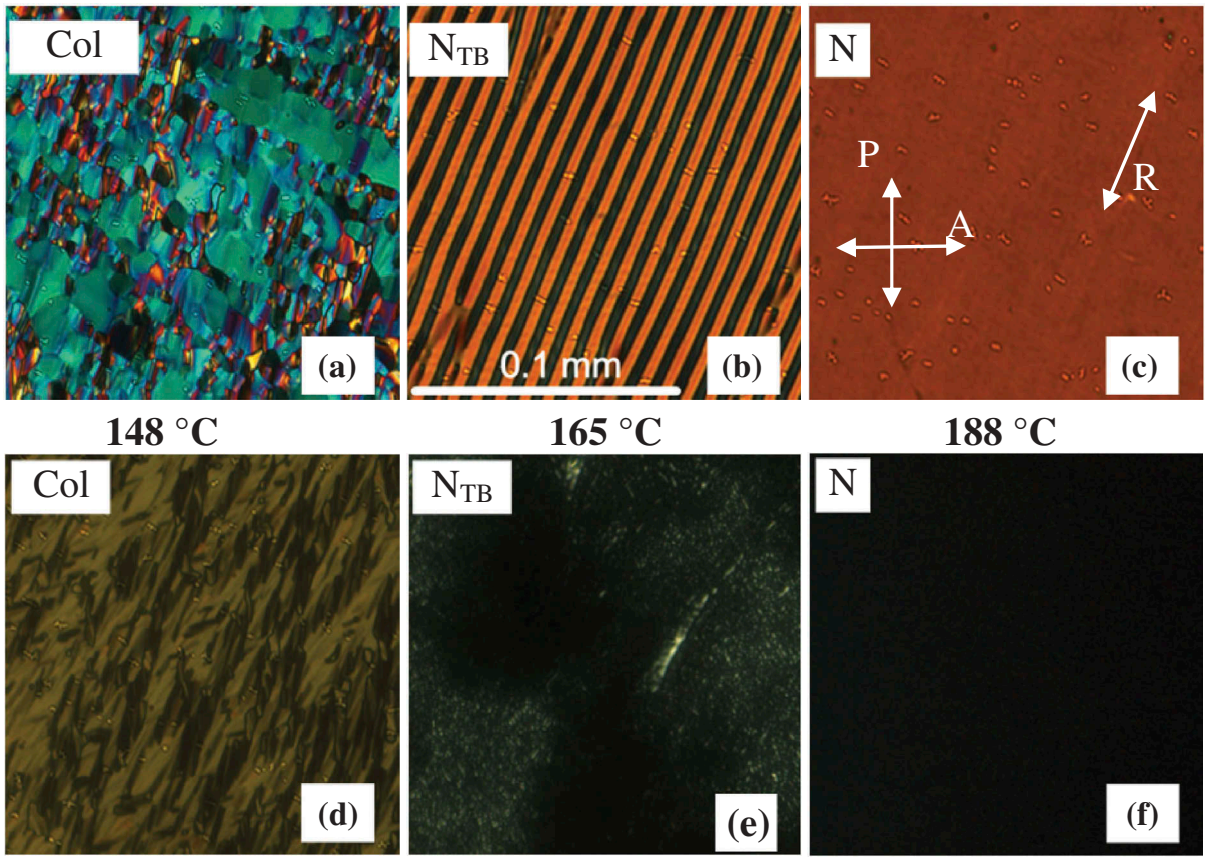

Figure 2. Polarising optical microphotographs of the planar (cell gap 4 μm) (a) to (c) and homeotropic (cell gap 6 μm) cells (d) to (f). (a, d) correspond to the columnar phase, (b, e) correspond to the N_{TB}, and (c, f) correspond to the high-temperature nematic phase. For both cells of planar and homeotropic alignments, the textures are recorded during the cooling process from the isotropic state.

[4]. Though the quality of homeotropic alignment for this material in N and N_{TB} phases is reasonably satisfactory, a fine network of defects is visible in the N_{TB} under high sensitivity camera settings (Figure 2(e)), which are similar to the dimer-based N_{TB} phase. The textures exhibited in Figure 2(a,d) correspond to that of the columnar phase, observed in between the temperatures of 150°C and 135°C.

The N_{TB} phase in this bent-core material exhibits most of the observed features of such a phase of the dimers. In addition to the observed striped texture, the domains of opposite handedness (Figure 3(b,c)) are observed;

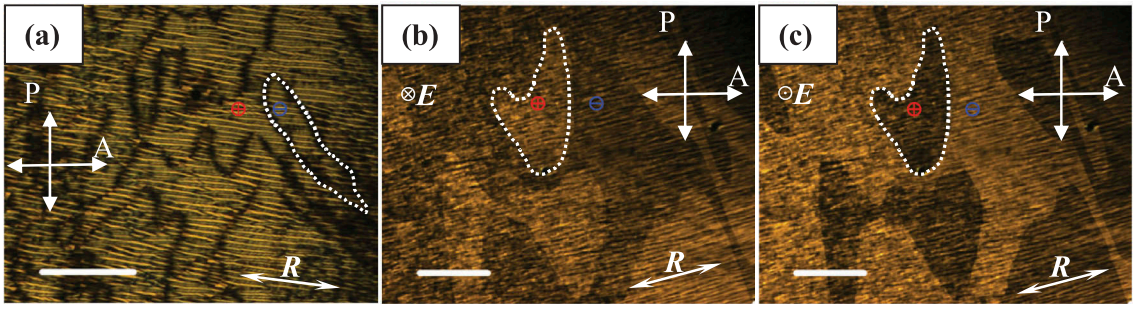

Figure 3. POM textures in the N_{TB} phase of a 3 μm planar cell. Scale bars are 100 μm long. The rubbing direction is adjusted between the polarisers in order to achieve the best contrast of the image. (a) No field applied across the cell; self-deformation stripes are formed with chiral domains of opposite handedness designated by Red ⊕ and Blue ⊖. (b, c): ±40 V_{DC} are applied across the cell. The self-deformation stripes are suppressed; domains of opposite chirality are clearly identified by applying the electric field of the opposite polarity.

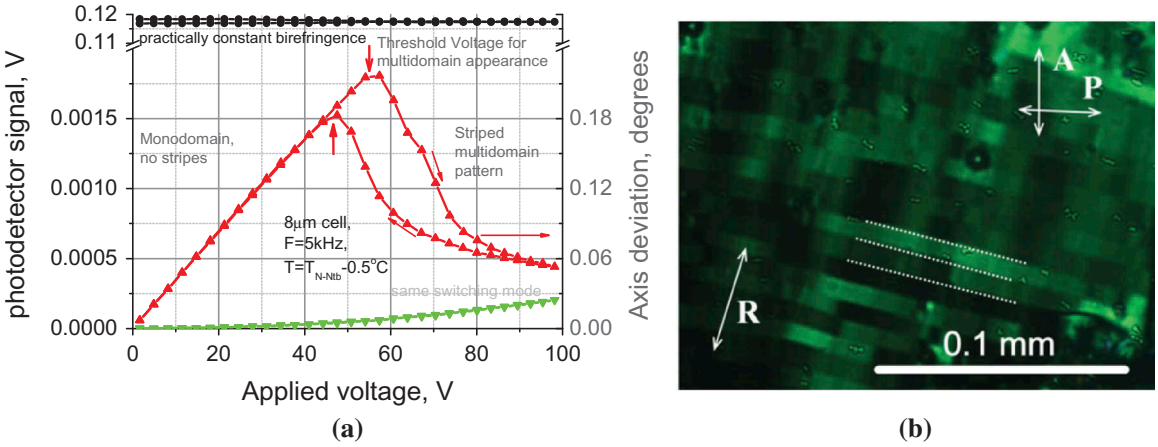

Figure 4. (Colour online) Field-induced domains of opposite handedness. (a) Threshold behaviour of the domains, planar 8 μm cell, 100 s/point, 5 kHz, sine wave. The amplitude of the first harmonic Red (▲) indicates that multi-domains appear at 6.9 V/μm [55.2 V on the graph] (red arrow down) on increasing the electric field and disappear at 5.6 V/μm [44.8 V on the graph] (red arrow up) when the field is decreased. The in-plane deviation of the optical axis $\psi = \frac{V_{1f}}{4V_{DC}}$ is scaled on the right-hand-side axis of the figure. Note that the DC component (●) is practically constant indicating no major change in the birefringence and therefore no electro-convection. The second harmonic signal Green (▼) is independent of the chirality handedness of domains and increases with field after domains are formed. (b) Polarising optical microphotograph of the domains texture observed in a 12.6-μm one-sided rubbed planar cell, 60 kHz, applied sine wave 75 V_{0-Pk}. Some of the domain boundaries are highlighted with dotted lines.

handedness of domains is verified by applying an external alternating electric field [2]. Chirality in homeotropic cells is observed by de-crossing the polarisers on both sides. Domain boundaries are observed by discontinuities in the self-deformation striped pattern recorded even without applying an external electric field (Figure 3(a)). For relatively weak externally applied electric fields across the cell, domains are possibly dictated by the thermal prehistory of the sample (Figure 3), while they will transform to a striped pattern (i.e. patterns in Figure 3(b) and 3(c) will change to Figure 4(b)) [3] when high-frequency electric field of a large enough amplitude is applied across a planarly aligned cell.

The switching time of the oblique helicoid structure is given by

$$\tau = \frac{\gamma p^2}{4\pi^2 K \sin^2\theta_0}, \quad (1)$$

τ is proportional to the second power of the helical pitch and is inversely proportional to the sine squared of the heliconical angle. Tangent of the switching angle is given by $\tan\psi = \frac{eEp}{2\pi K}$ [19,20]. The switching time in the N_{TB} phase is found to change from 15 to 11 μs on cooling from temperature of 165°C to ~ 152°C. This result is in good qualitative agreement with a 20% decrease of the nanoscale helical pitch with a decrease in temperature by ~13°C reported recently [21]. The switching time for the bent-core system is of the same order but its magnitude is slightly lower than for dimers [2,20,22]. Furthermore, the electroclinic coefficient $\frac{\partial\psi}{\partial E} = \frac{ep}{2\pi K}$, in the approximation of small ψ, is found to be approximately the same 0.036–0.04°/(V/μm) as for dimers. One notes from Equation (1), the slower switching time in particular may indicate a lower value of the conical angle θ_0. This is in agreement with the conclusions derived from the birefringence measurements presented below. Here, p, γ, K, and e are the helical pitch length, the effective viscosity, the effective elastic constant, and the effective flexoelectric coefficient, respectively. The longer value of the pitch reported for this material [17] compared to the dimers may also contribute to the slower switching time, although a higher working temperature would lower the viscosity too.

2.2 The electro-optic effect

In order to study the switching phenomenon in the N_{TB} phase, the rubbing direction in the cell is rotated such that the rubbing direction is directed at an angle of 22.5° to the polariser. An AC signal is applied across the cell. The intensity of the transmitted light is measured by a photodetector connected to a multifunctional DAQ board (National Instruments, NI-USB 6216). The acquired signal is then decomposed into DC, first and the second harmonics using software algorithm for a lock-in amplifier. The harmonics signals are locked to the reference channel of the voltage generator. The constituents of the output are recorded as a function of the temperature of the cell and the

applied electric field. Since the cell is placed under crossed polarisers, the transmittance through a planarly aligned cell is given by Equation (2). Here, α is the angle made by the rubbing direction with the polariser; ψ is the switching angle induced by the electric field. The sign of ψ is dependent on the polarity of the field applied, d is the cell thickness, Δn is the birefringence, and λ is wavelength of the light. I_0 is the light source intensity, whereas the dark current of the photodetector is neglected.

$$T = I_0 \sin^2[2(\alpha \pm \psi)]\sin^2\frac{\pi d\Delta n}{\lambda}. \quad (2)$$

On assuming a constant value of Δn and by setting $\alpha = 22.5°$, we obtain

$$T \propto \sin^2(45° + 2\psi) = \frac{1}{2}(1 + \sin(4\psi)). \quad (3)$$

On the assumption of a small value of ψ, one can easily separate out the unknown values of I_0 and Δn. If V_{DC} is the DC component and V_{1f} is the first harmonic of the applied signal, the photodetector response is given by $\psi = \frac{V_{1f}}{4V_{DC}}$.

For a general experiment, signal for the light passing through the domains of opposite chirality is mixed at the photodetector. Consequently, the first harmonic signal from the domain is dependent on chirality handedness and due to opposite handedness these cancel out with each other. However, in some cells, the size of one of the domains is large enough so as to cover the entire field of view of the microscope. In such a case, one can use the sample cell to investigate the switching and the threshold behaviour of the domains. Data for the components of the response signal as a function of the applied voltage are shown in Figure 4(a), where the scale on the right-hand side represents the values of ψ as obtained above. The first harmonic is seen to increase linearly with the applied field (field = voltage/thickness of the cell). The magnitude of the slope is $\frac{\partial\psi}{\partial E} = 0.036°\mu m/V$ which is close to the value of $0.04°\mu m/V$ previously found for the bimesogens [2,3,20,22].

When a field is increased to the threshold (indicated by a vertical red arrow in Figure 4(a)), the multi-domain striped pattern emerges from a single domain. The switching direction of the neighbouring domains implies that these are of opposite chirality. The domains form a striped pattern with a periodicity of several micrometres normal to the rubbing direction (***R***). The first harmonic signal from two domains of the opposite handedness cancels out, hence the first harmonic signal from the photodetector drops rapidly with an increase in the electric field as shown. Meanwhile, the second harmonic signal, arising from a change in the birefringence under large electric fields is not sensitive to the direction of the optical axis deviation and this continues to increase with increase in the field (Figure 4(a)). This indicates that the switching phenomenon itself is present well beyond the fields required for the onset of the striped multi-domain pattern.

For the bent-core system, the domain onset threshold near the transition to the nematic phase is almost two times lower compared to that previously determined for the dimers and their mixtures with monomers [3]. This result is also in agreement with the lower values of the heliconical angle found in this material. The lower angle implies lower domain wall energies thus allowing walls normal to the helical axis to form under lower external fields. This may be related to the higher working temperatures of this material and consequently to its lower viscosity.

There is also a noticeable hysteresis seen in the domain pattern formed under the electric field: on decreasing the field, the first harmonic signal corresponding to the mono-domain sample is restored at a field of approximately 20% lower than on increasing the field. These results are recorded at low enough speed, allowing for a settling time of 100 s for each voltage step across the cell. This is to negate possible contributions to the observed hysteresis from the viscosity in the N_{TB} phase. Figure 4(b) illustrates texture from domains in a planar cell. In order to generate an optical contrast between the neighbouring domains, asymmetry was introduced to the cell by rubbing only one of the two substrates. The direction of the stripes is found to be normal to the rubbing direction and the domains appear uniform along the rubbing direction with sharp boundaries between the two neighbouring ones. The green colour of the texture (Figure 4(b)) is due to the birefringence of the sample.

The negative dielectric anisotropy of the material causes Freedericksz transition in the homeotropic cells to occur. The non-aligned planar textures generated under the electric field are presented in Figure 5. One can clearly differentiate the typical Schlieren texture of the N phase from the N_{TB} phase (Figure 5(a)). The domains of opposite handedness [3] can also be induced by a large high-frequency electric field applied across such a cell (Figure 5(b,c)). However, they do not form uniformly aligned pattern since the surfaces of the cell do not have easy axis or axes as in the case of a planarly rubbed cell. Meanwhile, the domain boundaries are still normal to the local average director. On comparing Figure 5(b,c), one can see that the domain size decreases with increasing frequency of the applied

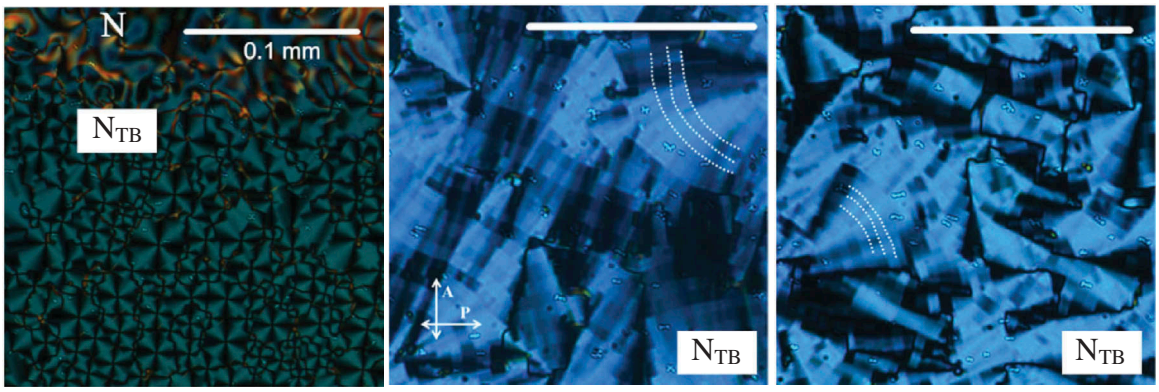

Figure 5. (Colour online) Microphotographs of 4 μm homeotropic cell under electric field. (a) 22 V_{0-Pk}, square wave, f = 1.4 kHz, N–N_{TB} phase transition (b) 76 V_{0-Pk}, sine wave, f = 20 kHz, N_{TB} close to the transition to N phase. Domains of opposite handedness are clearly visible under stroboscopic illumination. (c) An application of 76 V_{0-Pk}, square waveform signal, f = 45 kHz, the higher frequency of the applied signal leads to narrower stripes. Scale bars of all images are 0.1 mm across the microphotographs. Some of the domain boundaries are highlighted with dotted lines.

electric field. This is in line with the earlier observations for a dimer LC mixture [3,22]. The blue colour in Figure 5(b,c) arises from a combination of the sample birefringence and a 'cool white' spectrum of the stroboscopic LED light source used under which these are observed. The stroboscopic illumination is needed since the signal frequency for the formation of domains is much higher than the ordinary video frame rate of the camera used. Altering the phase between the illumination and the field applied to the sample causes interchange of the brightness of the neighbouring domains helping to identify the phenomenon.

2.3 Conical angle determined from the birefringence measurements

The birefringence, Δn, is measured in a planar cell by recording the transmittance spectra while keeping the cell at an angle of $\alpha = 45°$. The transmitted light through the LC cell between the crossed polarisers as a function of wavelength from Equation (2) is given as:

$$T = A \sin^2\left(\frac{\pi \Delta n_{\text{eff}} d}{\lambda}\right) + B. \quad (4)$$

Here, A is the scaling factor, Δn_{eff} is the effective birefringence, λ is the wavelength of light, d is the cell thickness, and B is the offset signal. The transmittance spectra are fitted to Equation (4), while the wavelength dependence of Δn is given by the extended Cauchy equation [23,24], Equation (5) is substituted in Equation (4)

$$\Delta n_{\text{eff}}(\lambda) = k_{\text{eff}}\left(\frac{\lambda^2 \lambda^{*2}}{\lambda^2 - \lambda^{*2}}\right). \quad (5)$$

Here, k_{eff} and λ^* are the parameters obtained from a detailed fitting of the transmittance to λ at one of the temperatures. The further fitting is carried out on the assumption that λ^* is a constant over the temperatures investigated.

Figure 6(a) shows the determined values of Δn as a function of temperature obtained using this fitting procedure. Measurements are carried out under cooling of a 9 μm planar cell filled with the bent-core compound. The magnitude of $\Delta n_{\text{eff}}(\lambda)$ is increasing with a reduction in temperature. The value of Δn in the nematic phase increases from 0.0779 (at 187°C) to ~0.1068 (at 167°C) due to an increase in the nematic order during the cooling cycle. Birefringence values are comparable to the values found for the ordinary nematic materials and in the nematic phase of the odd-linked dimers. Δn (T) in the vicinity of N–N_{TB} transition is magnified and given in the inset figure of Figure 6(a). This shows two transitions. One is related to the nematic to non-striped N_{TB} at 166.5°C (Δn = ~0.1074). Though a change in Δn is rather small (~0.001), it is still observable. The other transition is from non-striped N_{TB} to striped N_{TB} occurring at a temperature of approximately 165°C. On transition to the striped N_{TB} texture at 165°C, the effective birefringence starts to decrease. This is due to the spontaneously formed stripes by self-deformation.

Figure 6(b) shows the polarising microscopic texture corresponding to the birefringence study. The slight temperature gradient allows one to observe simultaneously textures of the classical nematic, high-temperature non-striped N_{TB} and the lower temperature striped N_{TB} phases. The textures are recorded on a 15 μm planar cell under cooling by keeping the cell at

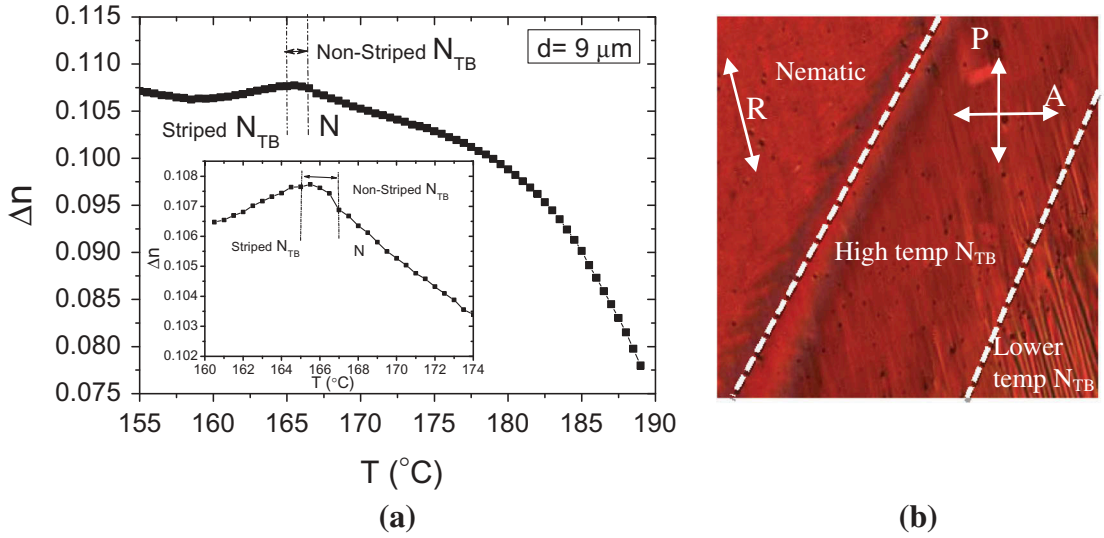

Figure 6. (Colour online) (a) The birefringence, Δn, in the N and N_{TB} phases plotted as a function of temperature in the absence of electric field. The inset figure of (a) shows Δn magnified in the vicinity of N–N_{TB} transition to show the jump in Δn under cooling. The measurement is carried out on a 9 µm planar cell by keeping the cell at an angle of α = 45°. (b) Polarising optical microscopic texture of the bent-core compound filled with a temperature gradient in a 15 µm planar cell shown for the phase transition of classical nematic to high-temperature non-striped N_{TB} and to the lower temperature striped N_{TB} textures are recorded under cooling by keeping the cell at an angle of α = 22°.

an angle of α = 22°. Although the actual director structure in the N_{TB} phase is rather complicated [9] and requires further investigation, but here we can estimate an apparent average deviation of the N_{TB} director from the one in the nematic phase (rubbing direction). According to the equation for conical angle θ_0 derived in [1],

$$\Delta n_{N_{TB}} = \Delta n_{extr}\left(1 - \frac{3}{2}\theta_0^2\right). \quad (6)$$

Δn_{extr} is the extrapolated value of the birefringence at a particular temperature, if transformation from the N phase to the N_{TB} had not occurred. $\Delta n_{N_{TB}}$ is the measured value at a temperature of interest. Δn_{extr} is obtained from the Haller's formula [28],

$$\Delta n_{extr} = \Delta n_0\left(1 - \frac{T}{T^*}\right)^{\beta}, \quad (7)$$

where the parameters Δn_0, T^*, and β are obtained by fitting the experimental birefringence data acquired in the high-temperature classical nematic phase. Here, Δn_0 corresponds to the birefringence value at the absolute zero temperature, T^* is the temperature of Iso–N phase transition, and β is a critical exponent. After determining these parameters, we can obtain Δn_{extr} for temperatures corresponding to the N_{TB} phase using Equation (7) and then obtain θ_0 using Equation (6). This procedure is verified using a classical dimer material and shows the value of θ_0 = 31°±3° for CBC7CB at 6°C below the N–N_{TB} phase transition. The heliconical angle found for CBC7CB here is in good agreement with the previous values reported in the literature for dimers [25–27].

Figure 7(a) shows the heliconical angle, θ_0, of the N_{TB} phase as a function of the reduced temperature which is determined from the Δn measurement using Equation (5). The inset in Figure 7(a) shows the temperature-dependent Δn for the high-temperature classical nematic phase fitted to the Haller's formula (Equation (7)), resulting in Δn_0 = 0.128, β = 0.145, and T^* = 188°C corresponding to the isotropic–N transition.

The maximum heliconical tilt angle determined by the above procedure in the N_{TB} phase of the material under investigation is approximately 9.3° at the lowest temperature of measurement.

3. Conclusions

In summary, the characteristic properties of N_{TB} phase of an asymmetrical achiral rigid bent-core LC, terminating in symmetrical alkyl chains (R_1=R_2=OC_6H_{13}) are reported. The main reason for forming the N_{TB} phase in this case seems to be the asymmetry of the molecule. It is noted that the twist-bend nematic phase is observed in rather few bent-core systems. The only other known example is that of an elongated structure of a bent-core system investigated recently by Wang et al. [29]. The main characteristics are similar to that of dimer connected with an odd number

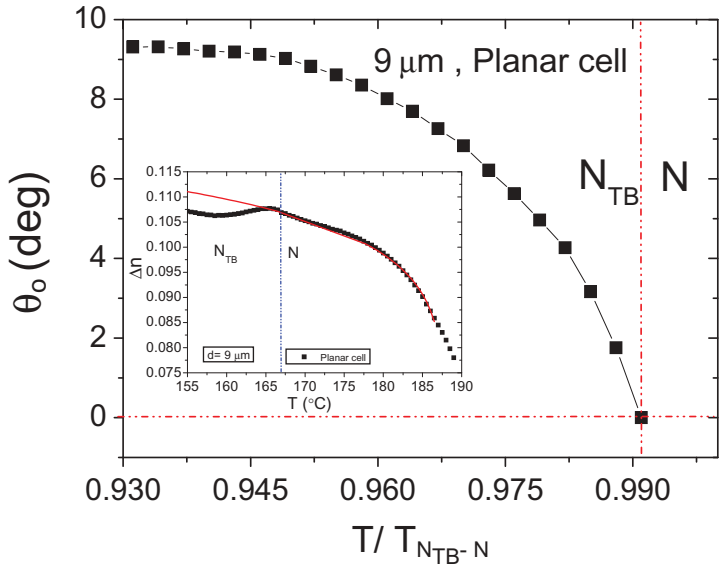

Figure 7. (Colour online) Heliconical angle, θ_0, in the N_{TB} phase observed in the bent-core compound as determined from the Δn measurements as a function of the reduced temperature. The inset shows the temperature-dependent experimental Δn (■) and (red line) shows fitting of the data to the Haller's equation. Birefringence measurements are carried out on a 9-µm planar cell under cooling by keeping the cell at an angle of α = 45°.

of methylene units. This implies that main characteristics of the twist-bend nematic phase apart from the heliconical angle are independent of the material so long as the material exhibits the twist-bend nematic phase. The question as to why very few bent-core systems exhibit N_{TB} phase needs to be further examined. It would appear that the molecule should be able to twist and bend but more importantly should have lower values of K_{33} and K_{22} and these must be lower than K_{11} [30,31]. The nematic–nematic phase transition and its characteristics are investigated using DSC, polarising microscopy, and electrooptics. At zero external field, the periodic stripes are spontaneously formed and these are parallel to the rubbing direction, their periodicity is related to the cell thickness. The onset of the periodic striped domains of the opposite handedness with sharp boundaries for higher amplitudes of AC electric field for this bent-core compound is found to be similar to those in difluoroterphenyl dimers. This appears to be an important consequence of the model proposed by Dozov for the N_{TB} phase, which is supported by our experimental results.

The Haller's extrapolation technique for extrapolating the birefringence is used to determining the temperature dependence of the conical angle. This achiral bent-core LC shows lower values of the heliconical angle (~9.3° at 155°C) as compared with a conventional twist-bend nematic phase of achiral dimers (31°±3°). This lower value of the heliconical angle is in qualitative agreement with (a) the slower response, (b) the lower threshold field required for the formation of the striped pattern of domains of opposite handedness, (c) the lower value of the enthalpy for the N–N_{TB} phase transition. Future investigations may include determining the values of the flexoelectric, elastic, and viscosity coefficients for carrying out a detailed investigation for arriving at a better understanding of the phenomena involved.

Acknowledgements

G Shanker thanks Dr C V Yelamaggad *et al.* of the Centre of Nano-science and soft matter research (CeNS), Bangalore for using their laboratory facilities.

Disclosure statement

No potential conflict of interest was reported by the authors.

Funding

This work is supported by 13/US/I2866 from the Science Foundation Ireland as part of the US–Ireland Research and Development Partnership programme jointly administered with the United States National Science Foundation under Grant Number NSF-DMR-1410649.

References

1. Borshch V, Kim Y-K, Xiang J, et al. Nematic twist-bend phase with nanoscale modulation of molecular orientation. Nat Commun. 2013;4:2635–2643. DOI:10.1038/ncomms3635

2. Panov VP, Balachandran R, Nagaraj M, et al. Microsecond linear optical response in the unusual nematic phase of achiral bimesogens. Appl Phys Lett. 2011;99:261903. DOI:10.1063/1.3671996
3. Panov VP, Balachandran R, Vij JK, et al. Field-induced periodic chiral pattern in the Nx phase of achiral bimesogens. Appl Phys Lett. 2012;101:234106. DOI:10.1063/1.4769458
4. Panov VP, Nagaraj M, Vij JK, et al. Spontaneous periodic deformations in nonchiral planar aligned bimesogens with a nematic-nematic transition and a negative elastic constant. Phys Rev Lett. 2010;105:167801. DOI:10.1103/PhysRevLett.105.167801
5. Tripathi CSP, Losada-Perez P, Glorieux C, et al. Nematic-nematic phase transition in the liquid crystal dimer CBC9CB and its mixtures with 5CB: A high-resolution adiabatic scanning calorimetric study. Phys Rev E. 2011;84:041707. DOI:10.1103/PhysRevE.84.041707
6. Chen D, Porada JH, Hooper JB, et al. Chiral heliconical ground state of nanoscale pitch in a nematic liquid crystal of achiral molecular dimer. PNAS. 2013;110:15931–15936. DOI:10.1073/pnas.1314654110
7. Meyer RB. Structural problems in liquid crystal physics. In: Balian R, Weil G, editors. Les Houches summer school in theoretical physics, 1973. Molecular fluids. New York (NY): Gordon and Breach; 1976. p. 273–373.
8. Dozov I. On the spontaneous symmetry breaking in the mesophases of achiral banana-shaped molecules. Euro Phys Lett. 2001;56:247–253. DOI:10.1209/epl/i2001-00513-x
9. Panov VP, Varney MCM, Smalyukh II, et al. Hierarchy of periodic patterns in the Twist-bend nematic phase of mesogenic dimers. Mol Cryst Liq Cryst. 2015;611:180. DOI:10.1080/15421406.2015.1030252
10. Cestari M, Diez-Berart S, Dunmur DA, et al. Phase behavior and properties of the liquid-crystal dimer 1″,7″-bis(4-cyanobiphenyl-4′-yl) heptane: A twist-bend nematic liquid crystal. Phys Rev E. 2011;84:031704. DOI:10.1103/PhysRevE.84.031704
11. Henderson PA, Imrie CT. Methylene-linked liquid crystal dimers and the twist-bend nematic phase. Liq Cryst. 2011;38:1407–1414. DOI:10.1080/02678292.2011.624368
12. Šepelj M, Lesac A, Baumeister U, et al. Dimeric Salicylaldimine-based mesogens with flexible spacers: parity-dependent mesomorphism. Chem. Mater. 2006;18:2050–2058. DOI:10.1021/cm0526213
13. Griffin AC, Britt TR. Effect of molecular structure on mesomorphism. 12. Flexible-center Siamese-twin liquid crystalline diesters - a “prepolymer” model. J Am Chem Soc. 1981;103:4957–4959. DOI:10.1021/ja00406a056
14. Attard GS, Date RW, Imrie CT, et al. Non-symmetric dimeric liquid crystals the preparation and properties of the α-(4-cyanobiphenyl-4′-yloxy)-ω-(4- n-alkylaniline-benzylidene-4′-oxy)alkanes. Liq Cryst. 1994;16:529–581. DOI:10.1080/02678299408036531
15. Imrie CT, Luckhurst GW. In: Demus D, Goodby JW, Gray GW, et al., editors. Handbook of liquid crystals. Vol. 2B. Weinheim: Wiley-VCH; 1998. ch. X.
16. Henderson PA, Seddon JM, Imrie CT. Methylene- and ether-linked liquid crystal dimers II. Effects of mesogenic linking unit and terminal chain length. Liq Cryst. 2005;32:1499–1513. DOI:10.1080/02678290500284983
17. Chen D, Nakata M, Shao R, et al. Twist-bend heliconical chiral nematic liquid crystal phase of an achiral rigid bent-core mesogen. Phys Rev E. 2014;89:0225067. DOI:10.1103/PhysRevE.89.022506
18. Schröder MW, Diele S, Pelzl G, et al. Different nematic phases and a switchable SmCP phase formed by homologues of a new class of asymmetric bent-core mesogens. J Mater Chem. 2003;13:1877–1882. DOI:10.1039/B305451A
19. Patel JS, Meyer RB. Flexoelectric electro-optics of a cholesteric liquid crystal. Phys Rev Lett. 1987;58:1538–1540. DOI:10.1103/PhysRevLett.58.1538
20. Meyer C, Luckhurst GR, Dozov I. Flexoelectrically driven electroclinic effect in the twist-bend nematic phase of achiral molecules with bent shapes. Phys Rev Lett. 2013;111:067801. DOI:10.1103/PhysRevLett.111.067801
21. Zhu C, Tuchband MR, Young A, et al. Resonant carbon K-edge soft X-ray scattering from lattice-free heliconical molecular ordering: soft dilative elasticity of the twist-bend liquid crystal phase. Phys Rev Lett. 2016;116:147803. DOI:10.1103/PhysRevLett.116.147803
22. Panov VP, Vij JK, Balachandran R, et al. Properties of the self-deforming Ntb phase in mesogenic dimers. Proceedings of SPIE 8828, Liquid Crystals XVII, 88280X; San Diego, CA, Aug 25, 2013.
23. Li J, Wu S-T. Extended Cauchy equations for the refractive indices of liquid crystals. J Appl Phys. 2004;95:896. DOI:10.1063/1.1635971
24. Panarina OE, Panarin YP, Antonelli F, et al. Investigation of de Vries SmA* mesophases, in low molecular weight organosiloxane compounds. J Mater Chem. 2006;16:842–849. DOI:10.1039/B509119E
25. Challa PK, Borshch V, Parri O, et al. Twist-bend nematic liquid crystals in high magnetic fields. Phys Rev E. 2014;89:060501 (R). DOI:10.1103/PhysRevE.89.060501
26. Meyer C, Luckhurst GR, Dozov I. The temperature dependence of the heliconical tilt angle in the twist-bend nematic phase of the odd dimer CB7CB. J Mater Chem C. 2015;3:318–328. DOI:10.1039/C4TC01927J
27. Robles-Hernández BR, Sebastián N, de la Fuente M, et al. Twist, tilt, and orientational order at the nematic to twist-bend nematic phase transition of 1″,9″-bis(4-cyanobiphenyl-4′-yl) nonane: A dielectric, H2NMR, and calorimetric study. Phys Rev E. 2015;92:062505. DOI:10.1103/PhysRevE.92.062505
28. Haller I. Thermodynamic and static properties of liquid crystals. Prog Solid State Chem. 1975;10:103–118. DOI:10.1016/0079-6786(75)90008-4
29. Wang Y, Singh G, Agra-Kooijman DM, et al. Room temperature heliconical twist-bend nematic liquid crystal. Cryst Eng Comm. 2015;17:2778–2782. DOI:10.1039/C4CE02502D
30. Balachandran R, Panov VP, Vij JK, et al. Elastic properties of bimesogenic liquid crystals. Liq Cryst. 2013;40(5):681–688. DOI:10.1080/02678292.2013.765973
31. Yun C-J, Vengatesan MR, Vij JK, et al. Hierarchical elasticity of bimesogenic liquid crystals with twist-bend nematic phase. Appl Phys Lett. 2015;106:173102–173105. DOI:10.1063/1.4919065